Strip Cooling Optimization by Means of Fully Coupled Thermo-Mechanical-Metallurgical 3D Model

J. H. Bianchi[1], L. Langellotto[1], J. Díaz Alvarez[2]

[1] Centro Sviluppo Materiali S.p.A., [2] Arcelor Mittal España S.A.

Abstract: Advanced High Strength Steels (AHSS) are the fastest growing segment of strip products due to their high demand in the automotive industry. Because they represents valid alternative to the use of expensive ferroalloys, steel producers are pushed to improve the processing routes and guarantee uniform properties conforming to specific targets.

During the cooling phase on the Run Out Table (ROT), thermal and phase transformation inhomogeneities throughout the strip could lead to some sectors of this not conforming to target mechanical properties. Moreover, the differential shrinkage between neighboring fibers might induce plastic deformation leading to permanent loss of flatness.

CSM metallurgical module microView^{TM} has been fully coupled in Abaqus/Standard Thermo-Mechanical analysis and used in 3D modeling under generalized cooling conditions. First, it was applied to simulate rolling experiments done at CSM pilot mill using different cooling rates; the predicted volume fraction of constituent phases were compared against Metallographic measurements with good agreement. Secondly, the model was applied to an Arcelor Mittal España SA industrial line configuration and a sensitivity analysis was carried out to assess the effect of different cooling rates at the upper and lower face of the strip and finishing mill conditions (Temperature and Austenite grain size) on both breakdown of constituent phases and flatness. The model can be effectively used to optimize industrial parameters to guarantee dimensional/microstructure uniformity and absence of flatness. Moreover, an "early-quick" strategy that involves finishing water cooling and coiling the strip earlier were also examined and industrial practice modified accordingly to the predictions, with improvements in the strip quality

Keywords: AHSS, Multiphase Steels, High Strength Steels, Hot Rolled Strip, Hot Rolling Technology, ROT, Run Out Table, Cooling bed, Coiling, Strip Flatness, Microstructural Coupling, Austenite Decomposition, Austenite Evolution, SRX, MDRX,DRX, Grain Size, Multiphase Properties.

1. Introduction

The industrial production of modern microalloyed Advanced High Strength Steels (AHSS) strips such as Partially Bainitic, Dual Phase, Multi-Phase or TRIP, poses stringent requirements not only to rolling technology but also on the development and control of key properties during the accelerated cooling that follows (Sellger, 2003; Ibrahim, 2007; Bhattacharya, 2010; De Moor, 2010; Li, 2010; Barbero, 2012). These AHSS strips are produced from as-cast stocks heavily reduced to typical final thickness of 3 to 5 mm and width 1.2-1.50 m by a sequence of several rolling passes in Austenite state, followed by controlled cooling at the Run Out Table (ROT) and coiling of the strip (Figure 1). Austenite decomposes at the ROT in Ferrite and depending on the Carbon content and cooling condition, into a number of harder secondary phases: Pearlite, Bainite, Martensite, leaving in some cases a small fraction of retained Austenite that improves cold work hardening characteristics by Transformation Induced Plasticity.

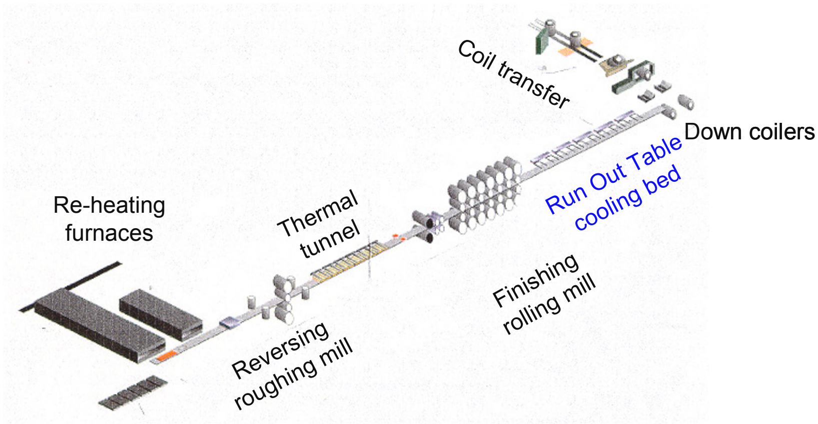

Figure 1. Typical Hot Strip Mill configuration

Mechanical properties are strongly dependent on chemical composition and on the volume fraction of constituent phases, as well as on specific parameters of each species (Sellger, 2003; Gutierrez, 2008; Bianchi, 2008): interlamellar space in Pearlite, grain size of Ferrite and Martensite, package size of Bainite, amount of retained Austenite, etc.. In turn, all these metallurgical variables are controlled by gross industrial parameters like number and position of active water jets and their flux rate, the strip traveling speed on the ROT and time at which water cooling is stopped to coil the strip.

AHSS is a growing segment of strip products, particularly because of their low cost, high strength and improved elongation to fracture (Bhattacharya, 2010; Li, 2010). Due to the narrow window of processing conditions imposed by the microstructure evolution during rolling and cooling, it can become very difficult to produce these grades industrially with a low disturbance rate. Thus, process parameters have to be optimized with tight criteria to satisfy customer tolerances in thickness, flatness, microstructure and mechanical properties.

During the hot rolling schedule, thickness, temperature, strain, its rate and hence microstructure differences appear through thickness and across the product width, not to mention length. Whilst technologies based on control by roll bending, skewing and thermal crown, intermediate roll shifting, etc can be effective in reducing thickness and flatness problems during the rolling stage, these reappears somehow again during cooling together with heterogeneous microstructure distributions because local thermal differences. An eventual cold rolling effort to correct thickness and flatness does not remove the spread in microstructure and hence in mechanical properties.

During cooling at the ROT, even the best performing water curtain/laminar adjacent jets configurations might introduce local variations in temperature between the strip top and bottom surfaces, as well as between middle width span and its borders. As a consequence, uneven solid state transformation patches might result across the product that would lead to undesirable differences in:

- the breakdown of constituent phase's volume fractions on samples taken at different locations, with the net result of mechanical properties not conforming to target specifications and tolerances.
- shrinkage between neighboring locations leading to a strip not conforming to flatness tolerances.

In order to minimize discards not conforming to the tight tolerances imposed, it is extremely important to know the reaction of the material to variations of the industrial parameters. Experimental monitoring on industrial lines by intermediate sampling is limited because of difficult accessibility and quenching times not short enough. In this context, a simulation using metallurgical knowledge from controlled mechanical testing and its validated extension to more general conditions, becomes a powerful tool to track the product evolution under realistic plant conditions. Meant as an off-line application, it can be used to study the effects of changing few industrial parameters at a time to achieve steel grade and quality targets.

One important feature of the ROT is the cooling system composed of several laminar and discrete water jets positioned along its length. Cooling from impinging water jets depends on the flow rate and depth of water accumulated on the moving strip. An experimental-numerical study on a single jet has indicated that whilst in general a deeper water pool on the top surface increases heat transfer, this becomes reduced for very deep pools because steam removal is more difficult (Cho, 2008). A detailed simulation of an industrial ROT configuration (Prieto, 2001) having several water curtains/adjacent and discrete jets on the strip upper face and only jets on the lower face, determined heat transfer coefficients in terms of water flow rate and its impact speed that gave ending temperatures (strip coiling start) matching very well pyrometer data. Thermo-Physical bulk properties, however, were used without a detailed link to the evolving phase transformations. A fast one dimensional model (Ibrahim, 2007) for ROT cooling to produce AHSS incorporates Austenite decomposition and temperature evolution down to coiling. The ROT model presented herein covers all these features and additionally computes explicitly Thermo-Physical properties from constituents and their volume presence in the Multiphase steel. Moreover, it is three dimensional, which allows quantifying and controlling undesirable non-uniformity of properties and loss of flatness.

A suite of steel microstructure models for hot deformation and solid state transformation developed and tested over the years by CSM, have been particularized in this work for a 0.07 % C, 1.4 % Mn, Nb-Ti microalloyed steel. The models have been interfaced to Abaqus/Standard, validated against experimental pilot mill rolling results and used for sensitivity studies of an Arcelor Mittal Spain hot strip industrial line.

2 Austenite evolution during multipass rolling

Mechanical testing by compression or torsion under isothermal, constant strain rate conditions involves strain Hardening (H), Dynamic both Recovery (DRV) and Recrystallization (DRX), this last if the accumulated strain ε exceeds a threshold:

$$\varepsilon_{dyn} = F(T, \varepsilon, \dot{\varepsilon}, AGSo, Nb, Ti) \quad (1)$$

which depends on the temperature T, strain rate $\dot{\varepsilon}$, initial Austenite Grain Size $AGSo$ and microalloy content. Explicit expressions of ε_{dyn} for the Nb-Ti steel under consideration were taken from (Fernandez, 2003). DRX reduces the accumulated strain and generates a X_{DRX} volume fraction, normally cast as an Avrami equation in terms of strain [Bianchi, 2005]:

$$X_{DRX} = 1 - e^{k_d (\varepsilon / \varepsilon_{dyn})^{n_d}} \quad (2)$$

of small diameter grains [Roucoules, 1994;Fernandez, 2003]:

$$d_{DRX} = F(T, \dot{\varepsilon}) \quad (3)$$

Isothermal holding for a time t after deformation induces softening and strain release by either Static Recrystallization (SRX) or Metadynamic Recrystallization (MDRX):

$$X_{SRX,\,MDRX} = 1 - e^{k_{s,\,md} (t / t_{0.5})^{n_{s,\,md}}} \quad (4)$$

depending on whether the strain is below or over ε_{dyn}. Explicit Avrami equations in time for Equation 4 are normally obtained either by full stress relaxation or by double hit deformation after discrete holding times. The $t_{0.5}$ parameter is the time for 50% recrystallization, of the general form:

$$t_{0.5} = F(T, \varepsilon, \dot{\varepsilon}, AGSo, Nb, Ti) \quad (5)$$

for SRX (Fernandez, 2000), whilst no $AGSo$ or ε influence MDRX (Roucoules, 1994;Uranga, 2003). Post-deformation holding generates other two volume species, with different grain sizes, for the Nb-Ti steels:

$$d_{SRX} = F(\varepsilon, AGSo) \qquad \text{(Abad, 2001)} \quad (6)$$

$$d_{MDRX} = F(T, \dot{\varepsilon}) \qquad \text{(Urangam, 2003)} \quad (7)$$

Recrystallized fractions have a characteristic time $t_{0.99}$, past which grains grow:

$$AGSe = F(d_{SRX} \quad or \quad d_{MDRX}, T, t - t_{0.99}) \quad (8)$$

with different parameters for SRX and MDRX (Di Nunzio, 2000).

Incomplete recrystallization leaves elongated grains and their effective size can be determined as (Anelli, 1992):

$$AGSu = 1.06 \quad AGSo \quad e^{-\varepsilon} (1 - X)^{1/3} \quad (9)$$

After a given holding time t, three recrystallizing-growing species (Equations 3, 6, 7) of round grains, some of them grown as Equation 8 and a remaining fraction of deformed grains will be in general present. A subsequent deformation will result in a similar cycle for each of these families, generating a multiple structure of vanishing volume fractions. As the multiplicity after a sequence of interrupted deformation becomes too high, some merging criteria has to be selected (Sellars, 1986-1990; Bianchi, 1997;Langellotto, 2008a) to obtain after each pass a reduced set:

$$< AGS_e >= \text{average} \quad AGS_e \tag{10}$$

merged in terms of similar sizes. For most industrial cases, the spread reduces at the end of the rolling schedule, and a single representative mean average $< AGS_e >$ value can be obtained.

Industrial hot rolling inevitably introduces localization of strain rate and non-isothermal conditions. Should a FEM full resolution be needed, both integration of DRX contributions under varying strain rate and temperature conditions [Bianchi, 2005], as well as representative strain rate for the post-deformation $t_{0.5}$ (Equation 5) of the solid traveling in the interpass is required [Bianchi, 2009-2011]. In many cases this effort is not justified and a simplification is possible by using mean grain size values and isothermal homogeneous deformation models to calculate the microstructure at the entrance of a subsequent pass. The selection of the adequate modeling strategy depends on the finishing temperature and level of alloying: in their lower range of the first and high value of the second, detailed upstream microstructural history becomes more important and might require at least to FEM-model the last few passes. The multiple-microstructures simulation is equally important, and in this area CSM has developed and calibrated models over years of Steel Research using an extensive database of own and literature mechanical tests/plant data.

3. Isothermal austenite decomposition

TTT diagrams are produced by steel samples austenitized and then fast cooled to a lower Temperature that is kept constant while the rate of transformation in time is determined by Dilatometry. The Austenite isothermal decomposition into Ferrite, Pearlite and Bainite is characterized by incubation times during which atoms diffuse to form stable nuclei of the new phase and this then grows with the passage of time. The volume fraction of a secondary phase is normally expressed as an Avrami type of equation in time t [Anelli, 1989; Agarwal, 1981; Jia, 2010]:

$$X = 1 - e^{b(T) t^{n(T)}} \tag{11}$$

in which the b and n coefficients are calculated from the transformation start and finishing points on the TTT diagram, which are AGS_e -dependent.

The Martensitic transformation is time independent and its volumetric fraction depends only on the temperature [Koistinen, 1959]

$$X = 1 - e^{-0.011(Ms - T)} \tag{12}$$

4. Continuous Cooling Transformations

CCT diagrams normally obtained from controlled dilatometric experiments at ‘representative’ constant cooling rates can give a general indication on the evolution of the new phases. However, they cannot fully reproduce industrial conditions involving a continuum spectrum of Temperatures and variety of cooling rates imposed by the number of water curtains/laminar cooling and discrete jets alternating with radiation and boiling steam patches. In order to take full advantage of the resolution provided by the FEM models and to couple the mechanical, thermal and microstructural fields for industrial rolling applications, a hybrid experimental-modeling procedure has been developed that uses:

(a) As input experimental data from TTT isothermal transformation dilatometric diagrams. In absence of these, ‘derivate’ TTT diagrams can be obtained from experimental CCT data, by a reverse engineering procedure as detailed in §4.3.

(b) A General model for Continuous Cooling Transformation (Coppola, 1998a; Langelloto, 2008b)

(c) An Austenite Decomposition Model for coupled Temperature-Stress-Microstructural analysis (Coppola, 1998b; Langelloto, 2008b)

(d) A few experimental CCT continuous transformation dilatometric diagrams at constant cooling rate to calibrate the FEM implementation in steps (b) and (c) (Figure 2).

4.1 A General model for Continuous Cooling Transformation (GCCT)

In the general non-isothermal case, the given continuous cooling Temperarature-time profile is piece-wise split into the time intervals of the analysis.

For time-dependent transformations (Equation 11) an additivity principle (Scheil, 1935) is used to calculate the non-isotherm transformation starting time. The holding time Δt_i at a certain temperature divided by the time τ_i required for starting the transformation under isotherm conditions at that temperature represents the fraction of the total incubation time at that temperature. For non- isothermal cases, the transformation starts when the sum of the total incubation time fractions is equal to unity (Bhattacharya, 2010)

$$\sum_{i=1}^{m} \frac{\Delta t_i}{\tau_i} = 1 \tag{13}$$

During continuous cooling, the incubation times are in general longer than isothermally, because diffusion occurs at temperatures slowly decreasing. The time to form stable nuclei is then longer and the completion of the transformations requires more time.

The time-independent Martensitic transformation occurs when very fast cooling rates are applied and temperature falls below the M_s temperature. Austenite at these temperatures is no more stable and in absence of enough time for atomic diffusion distorts the lattice generating Martensite.

4.2 An Austenite decomposition model for coupled Temperature-Stress-Microstructural analysis: CSM microView™ module

The combined effects of thermal expansion and decomposition of Austenite entails volumetric changes that although small, become very important when accumulating as happens in several meters of rolled strip. The model considers:

- Changes in the crystalline lattice parameters that modifies Thermophysical properties as density, thermal expansion, conductivity, specific heat, elastic and plastic properties.
- Development of a multiphase microstructure, the hot strength of which varies with the state of the solid state transformations.
- Freeing latent heat that alters the thermal balance.

It follows that a realistic model aimed at industrial process simulation will have to involve not only capability to describe transformations under general cooling paths, but also to introduce multi-coupling between the microstructural predictions and both temperature and displacement fields. The Thermophysical properties then becomes time-Temperature dependent, because of the evolving transformations. A flexible FEM platform is required to link adequately all these features.

Models were implemented in Abaqus/Standard using the *COUPLED TEMPERATURE-DISPLACEMENT procedure. At the quasi-isothermal small time increments provided by the FEM analysis, the GCCT model is applied using TTT data as input to obtain transformed volume fractions and characteristics parameters of the constituent phases like interlamellar phase in Pearlite, Ferrite and Martensite mean diameters, Bainite package mean dimensions. Multiphase steel Thermo-Physical properties are then computed for the given temperature and time as volume-fraction weighed average of updated single constituent properties. The computed multiphase steel properties are collected from the GCCM-microView models in user subroutine USFLD and transferred to the material definition via both analytical coding in USER subroutines and DEPENDENCIES parameter in input cards.

4.3 Application of the FEM microView™ module to Mechanical Testing data

For the particular Nb-Ti steel under consideration, selected CCT diagrams at constant cooling rate were produced by Dr. Somani at Oulu University in a joint research project (Barbero, 2012). The constant cooling rate experimental conditions were next simulated by applying the model in §4.2, using brick and shell elements. By a reverse engineering procedure, trials TTT input data were then optimized till the transformation start and end Temperature-time points of the numerical simulation matched in the calibration CCT diagram (Figure 2). The resulting optimized TTT diagram is shown in Figure 3.

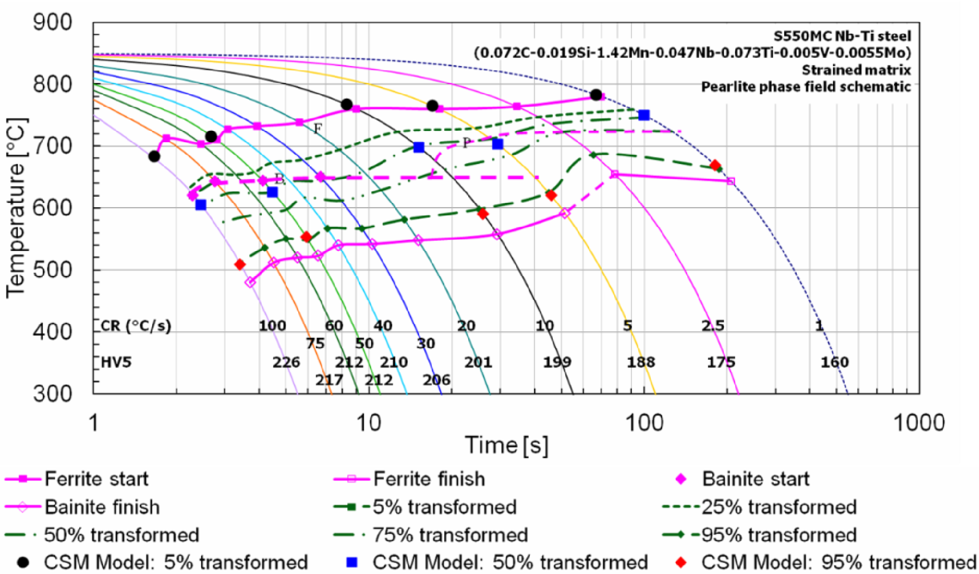

Figure 2. Comparison of experimental and predicted CCT diagrams at constant cooling rate, Nb-Ti steel

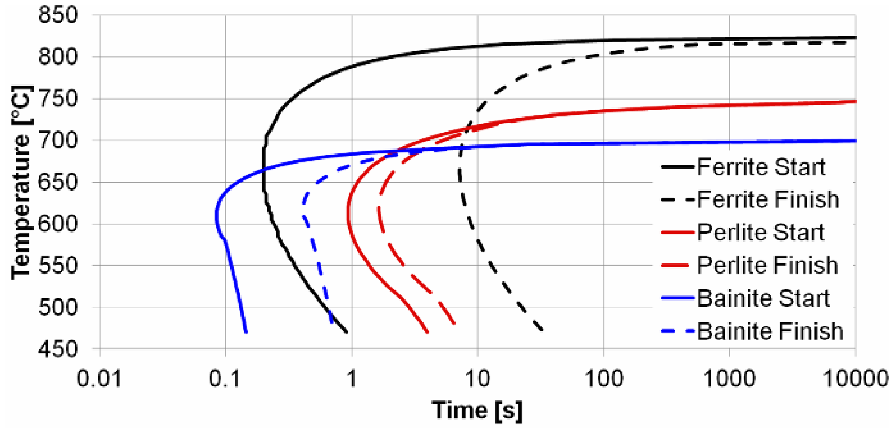

Figure 3. Optimized isothermal TTT derived from calibrating CCT diagrams at constant cooling rate, Nb-Ti steel

5. Validation of microView™ simulations with Pilot mill rolling experiments

Slabs 240 mm thick were soaked for 20 minutes at 1200°C, cooled down to a working temperature and then rolled at CSM pilot mill facility. Several experiments were done, with temperatures in the range 1000-1140 °C, strain accumulated in single and double passes between 0.3 to 0.9 and strain rates from 4 to 8 1/s (Table 1). The experiments were designed to induce Static and Metadynamic recrystallization conditions and obtain different grain sizes. Two Austenite mean grain size references were quenched: the prior to rolling $AGSo$ and the finish rolling $AGSe$.

Table 1. Experimental mill conditions and comparison of measured and predicted Austenite grain sizes at finish rolling.

R	vi	Hi	He	Ac	tc	Ω	r	ε	ε'	t	T	<Force> [t]		AGS_o	AGS_e [μm]	
[mm]	[m/s]	[mm]	[mm]	[mm]	[s]	[rpm]	[%]		[s^{-1}]	[s]	[°C]	Measured	Calculated	[μm]	Measured	Calculated
240	0.3	32	15.2	63.50	0.21	75	0.53	0.86	4.06	100	1136	55	56.7	89 ± 5	20 ± 5	24
240	0.3	32	15.5	62.93	0.21	75	0.52	0.84	3.99	100	1050	72	74.4	89 ± 5	18 ± 5	18
240	0.9	32	22	48.99	0.05	225	0.31	0.43	7.95	100	1053	46	44.4	89 ± 5	24 ± 5	28
240	0.5	32	24.5	42.43	0.08	125	0.23	0.31	3.63	20	1050	30	30.7	90 ± 5	-	33
		24.5	18.2	38.88	0.08	125	0.26	0.34	4.41	100	1000	40	39.9		20 ± 5	17
240	0.4	32	19	55.86	0.14	100	0.41	0.60	4.31	100	1138	50	47.6	88 ± 5	-	24
240	**0.6**	**32**	**22**	**48.99**	**0.08**	**150**	**0.31**	**0.43**	**5.30**	**20**	**1150**	**48**	**48.0**	**88 ± 5**	**-**	**28**
	0.6	**22**	**15**	**40.99**	**0.07**	**150**	**0.32**	**0.44**	**6.47**	**24**	**1076**	**54**	**55.4**		**-**	**16**
	0.6	**15**	**11**	**32.50**	**0.05**	**150**	**0.29**	**0.40**	**7.40**	**100**	**1005**	**67**	**69.2**		**20 ± 5**	**16**

Where:

R	Roll diameter [mm]	A_c	Contact arc length [mm]	ε	Strain	AGS_o	Prior austenitic grain size [μm]
Vi	Entry velocity [mm]	T_c	Contact time [s]	ε'	Strain rate [s-1]	AGS_e	Rolled austenitic grain size [μm]
Hi	Entry thickness [mm]	Ω	Roll speed [rpm]	t	Interpass time [s]	**Preconditioning for austenite decomposition model testing**	
He	Final thickness [mm]	r	Percentage reduction	T	Entry temperature at first pass [°C]		

Four cooling strategies were used at the ROT to produce different thermal profiles (Figure 4): in air, by laminar water jet and by fast immersion in both water and in a solution water-Aqua-Quench®; samples were taken for microstructural characterization.

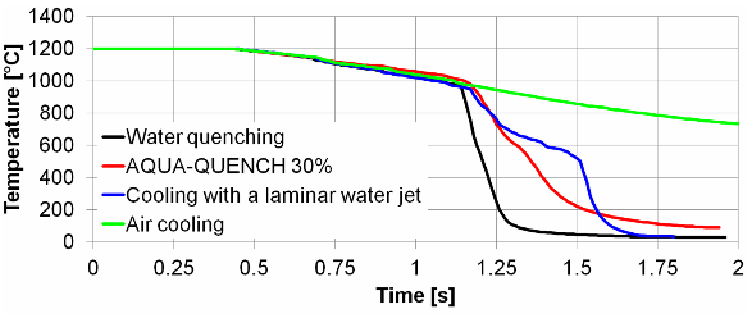

Figure 4. Resulting thermal cooling profiles after pilot mill rolling

The Austenite evolution model described in §2 was then applied using the prior $AGSo$ values and rolling conditions in Table 1 to obtain mean average $AGSe$. Comparison of these predictions against experiments shows good agreement. The FEM Austenite Decomposition model was next applied using as initial conditions the rolling exit grain size $AGSe$ together with the temperature and cooling profiles in Figure 4. Typical Multiphase microstructures after cooling and a comparison of predicted and Metallographic volume fractions are shown in Figure 5.

Phase	Quenching		AQUA-QUENCH 30%		Cooling with a laminar water jet		Air cooling	
	Measured	Calculated	Measured	Calculated	Measured	Calculated	Measured	Calculated
Ferrite	0.00%	2.00%	0.10%	2.00%	0.10%	1.00%	-	-
Perlite	-	-	-	-	-	-	6.00%	7.00%
Bainite	100.00%	91.00%	99.90%	98.00%	99.90%	95.00%	94.00%	93.00%
Martensite	0.00%	7.00%	-	-	0.00%	4.00%	-	-

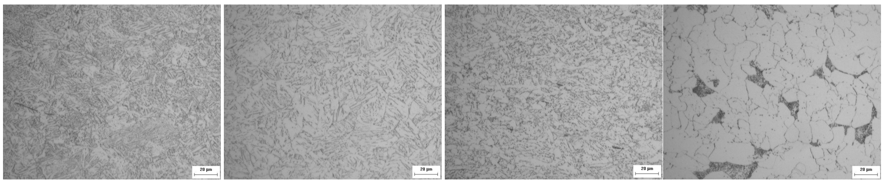

Figure 5. Comparison of microView^{TM} predictions and Metallographic measured multiphase volume fractions after pilot mill experiments. Nital etching, 50x mag.

6. Simulation of Industrial Cases

6.1 ROT model description

A FEM model for the strip Micro-Thermo-Mechanical evolution at the Run Out Table has been developed to predict the effects of different cooling schedules on both metallurgical properties and geometric changes using Abaqus/Standard. The microView™ model encapsulated in the Thermo-Mechanical analysis, previously validated by the calibrating CCT dilatometer tests (§4.3) and pilot mill rolling experiments (§5) is applied.

The rolled strip is modeled using 3D shell type linear elements S4T with full integration. The strip is kept fixed at the rolling end whilst the other one is pre-tensioned by a uniform specific load.

Initial conditions:

- across-width (Figure 7a) and through thickness Temperature and strain distributions
- across-width thickness profile of the hot rolled strip.

both of them numerically 'extruded' along the rolling direction. Estimates were obtained from the industrial plant, but eventually can be produced by a FEM simulation of the last rolling passes.

Variable loading conditions:

On its movement along the cooling bed, the strip undergoes several cycles of alternating heat losses by:

- Radiation and natural convection

- Forced convection by direct water impingement, with width-wise water curtains/laminar cooling by adjacent jets, distributed sweeping-water transversal jets in the upper face and angular jets on the lower face.
- Forced convection by boiling water accumulated at front and rear of jets/curtains.

which are introduced by defining localized surface-based non-uniform film coefficients along the strip by the card *SFILM and user subroutine FILM. The cooling system configuration is defined by in an auxiliary file ROT.dat that contains:

General data:

- ROT length, strip speed, number of cooling devices on the upper and lower strip faces, water flow rate and its sink temperature.

Upper face devices:

- identification number, initial position respect to strip fixed end.
- code type: water curtain, laminar cooling by adjacent jets, transversal water jet; status (open/closed)
- length on the strip of: water impingement zone, its stable boiling film zones at front and rear.
- selection of single or double impact area per device.

Lower face devices:

- identification number, initial position respect to strip fixed end
- code type: angular water jet; status (open/closed)
- water impingement length on strip.

These data are imported via user subroutine UEXTERNALDB and transferred via a common block to the FILM subroutine, where they are used to compute convective heat transfer coefficients (Figure 6). In the reference system fixed to the strip used, the original positions of cooling devices and associated areas are moved upstream at a velocity opposite to strip's.

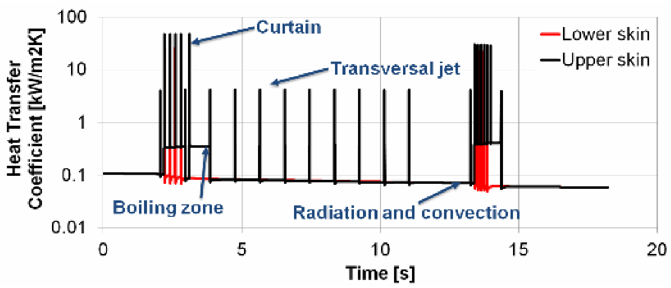

Figure 6. Typical heat transfer conditions on the industrial ROT

Convective cooling due only to water impact is the most effective term to drop temperature, with resulting film coefficients dependent on the impingement length determined by geometry of the cooling device, impingement water velocity and both water and strip temperatures (Prieto, 2001). The impingement velocity depends on the geometry of the cooling devices, on the distance and angle to the strip and on the water flow rate. The effects of all these gross industrial parameters, as well as the opening/closure of some cooling devices can be easily changed in the ROT.dat file specification.

Heat conduction to the ROT table rolls was neglected, on the assumption it is small because intermittent contact.

6.2 Validation of FEM Temperature predictions against industrial data

Figure 7b shows FEM predicted thermal rundown profiles along the ROT on strip mid-width at its core, upper and lower surfaces, and their validation against fixed pyrometers measurements and LandScan average on a monitoring length at Arcelor-Mittal Spain line. The marked temperature falls at discrete intervals correspond to the water impact followed by fast temperature recovery. The biggest falls corresponds to the laminar water cooling upper devices, which although are very effective can be seen to introduce differences between the strip upper and lower faces. Smaller temperature drops corresponds to the transversal jets cleaning redundant boiling water from the strip top surface.

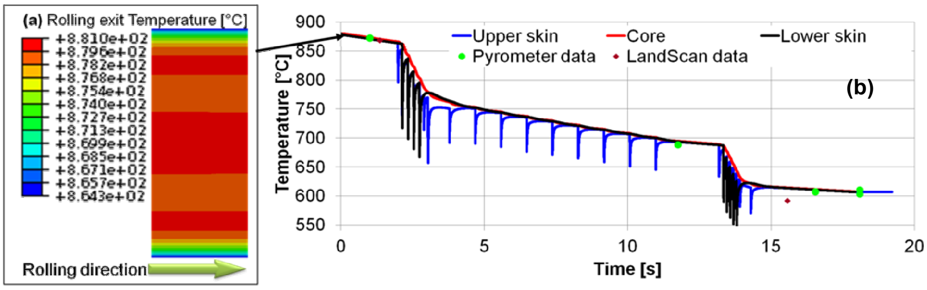

Figure 7. FEM predicted temperature profile at strip mid-width along the ROT and comparison with field measurements

6.3 Sensitivity of transformations to finish rolling temperature and rolled *AGSe*

Figure 8 shows FEM predicted volume fractions during Austenite decomposition along the industrial ROT, associated to the validated temperature strip mid-width rundown profile in Figure 7, for the Nb-Ti steel under study.

To assess the effects of finish rolling temperature and its *AGSe* grain size, these taken as initial conditions for the ROT simulation, the following hypothesis were examined:

(a) Conventional simulation using the industrial log data, with finish rolling conditions: mean temperature 880 °C and estimated AGS 30 microns.

(b) FEM simulation with the temperature as in (a), but with +/- 33% difference in *AGSe*

(c) FEM simulation with *AGSe* as (a) but with +/- 5 % difference in temperature.

A comparison of the through-thickness volume fractions (a) and (b) shows that for a given ROT exit time (coiling start), the remaining Austenite volume fraction decreases with the parent *AGSe* (Figure 9). The same trend is observed in Bainite, although the sensitivity disappears for *AGSe* above 30 microns. The resulting main phase Ferrite behaves the opposite way: its volume fraction decreases non-linearly with the increase of rolled grain size. Although the rolled *AGSe* has effect on volume fractions, its effects on the through-thickness distribution are minimal. Hot rolling control to achieve small *AGSe* is very effective in accelerating the Ferrite formation.

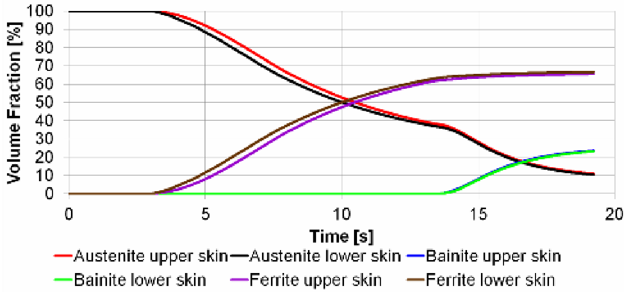

Figure 8. FEM predicted multiphase steel evolution along the industrial ROT for the thermal profile in Figure 7.

A comparison of the results for (a) and (c) shows that at equal ROT traveling time and fixed parameters of the cooling configuration, the rolling exit temperature modifies both the level of volume fractions and their through-thickness distribution. The higher the rolling temperature, the lower is the transformed phase's contents.

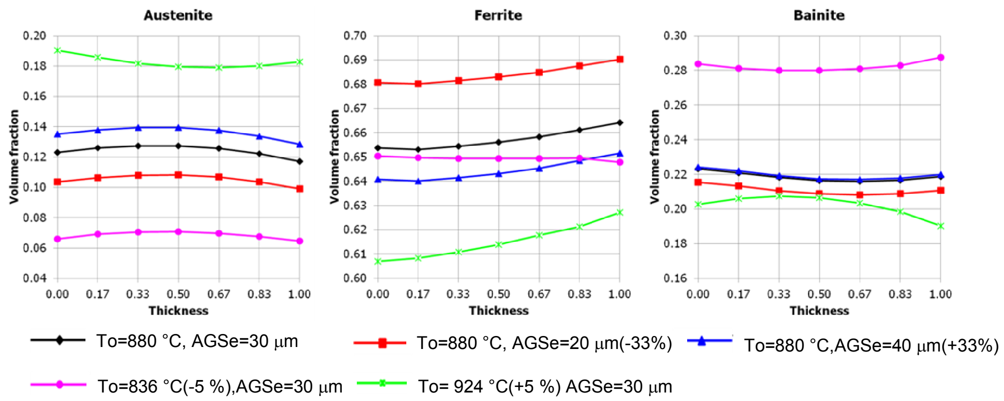

Figure 9. Comparison of through-thickness volume fractions predicted by conventional and full FEM simulations at different finish rolling temperatures and grain sizes (strip mid-width)

6.4 Sensitivity of transformations and flatness to cooling conditions

In order to validate the response of the FEM simulation to transformation shrinkage, industrial experiments were carried out modifying the water flow rate and active jets to induce significant material differences along cooling paths on strip faces and borders at the ROT end. The FEM simulation results for these conditions in Figure 10 clearly show that although at coiling start the temperature distribution on the strip is relatively uniform with no significant variation between its upper and lower surfaces, the different cooling conditions along the ROT have generated accumulation of unequal volume fractions on them.

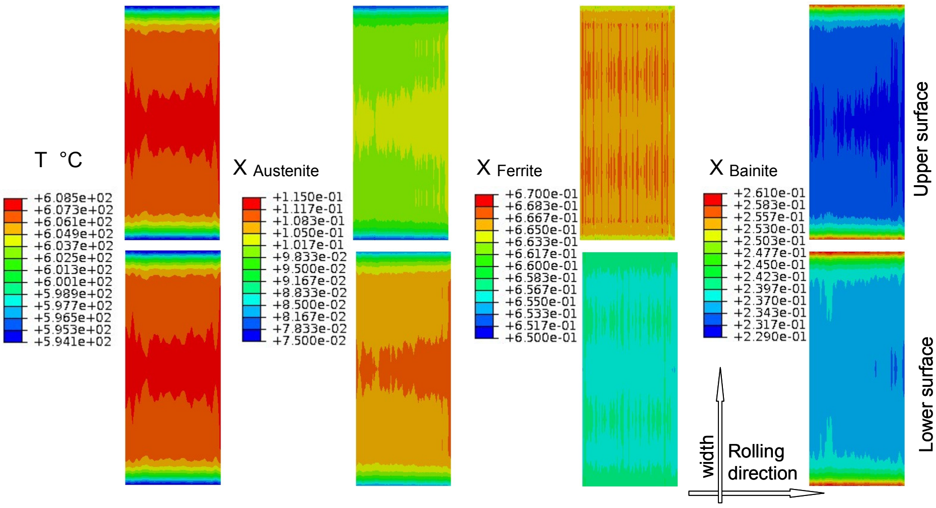

Figure 10. Comparison of predicted Temperature and Multiphase fractions at ROT exit (time=19.2 s)

During cooling, a density reduction occurs during Austenite decomposition, but this is overcome by its increase as temperature continues to drop; depending on the time stage, cooling first originates a volumetric expansion followed by a contraction. Along the same cooling path, the coefficient of linear expansion decays as temperature decreases, inducing a contraction. The more advanced the transformation becomes (less remaining Austenite), the higher the contraction. On release of strip frontal tension, the accommodation of residual stresses resulting from this differential shrinkage shortens the strip upper layers respect to the lower ones, with the net result of flatness loses (Figure 11). The modeling presented herein can quantify this deflection in terms of the gross industrial parameters defined in the ROT.dat file.

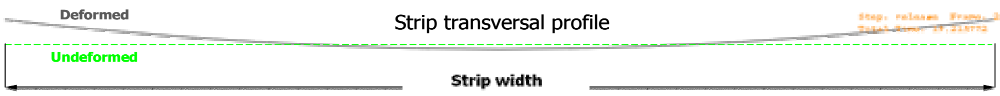

Figure 11. Strip flatness profile after removal of constraints for the conditions in Figure 10.

7. Optimization of industrial conditions

Figure 12 shows the application of the ROT simulation to two Case studies, starting from the same finish rolling temperature 900 °C, different cooling schedules and same coiling temperature. Case_1 fast ramp ends at 720 °C, slows down to 670 °C and is finally accelerated to 620 °C by activating an additional cooling section, while Case_2 main cooling stage finishes at 670 °C and then slows down to 620 °C. Figure 13 shows the through-thickness distribution of constituent volume fractions at the strip mid-width and border.

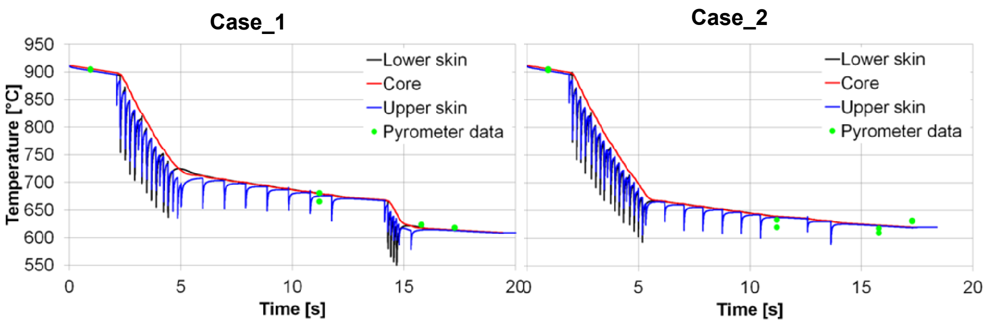

Figure 12. FEM cooling profiles at mid-width for two Case studies on the industrial configuration.

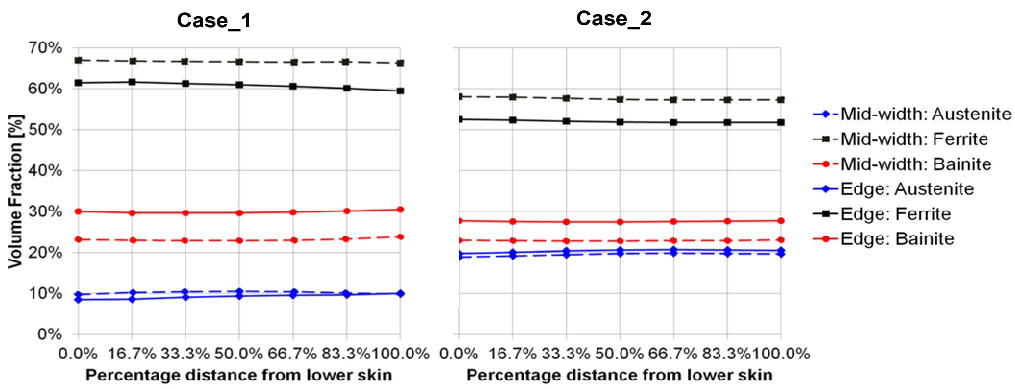

Figure 13. Predicted through-thickness multiphase volume fractions at strip mid-width and border for the 2 Case studies in Figure 12.

The resulting differential elongation between strip centre and edges is shown in Table 2. Although very small, the accumulation of this elongation differences along several meters of rolled strip represents a problem to flatness. In production terms, the 'absolute elongation' measure defined as $10^5 \Delta L / L_{reference}$ I-units is used, with ΔL being the difference between mid-width and border elongation over a reference length. $L_{reference}$. Rolled hot strip accepted good flatness quality should fall below 30 I-units.

Table2. Difference in border-center elongations for the 2 Case studies.

	Mid-width elongation %	Border elongation %	Flatness in I_units
Case_1	-0.244	-0.186	58
Case_2	-0.275	-0.238	37

Non-contact, laser-based flatness measurements systems are very expensive and because they are only effective where the tension due to coiling is not felt, are used only at the exit of the last finishing mill stand. Indirect methods commonly used are the observation of the videos taken in the coiling area, the falling of water over the bottom side inspection device and the instabilities in the coiling temperature. The videos only reveal flatness problems in severe cases and the last two methods only indicate the presence of water over the strip, but cannot guarantee that this presence is really linked to bad flatness.

In general, the coiling temperature appears more stable when water cooling is stopped earlier in the ROT. The use of the final "trimming" section (4 water nozzles at the ROT end, Case_1 in Figure 12) increases the risk of water accumulation and instabilities in the coiling temperature. The question that needs to be clarified is if the presence of water over the strip in the coiling area is really due to flatness problems or it is just because of the greater difficulty to remove water when using the last laminar cooling devices. Because risk of irregular temperature patches, an 'early quick' cooling strategy anticipating cooling appears in general very appealing for most microalloyed steels. For AHSS steels, this advantage in flatness has to be compatible with achieving the targeted breakdown of constituent phases (Figure 8) and their distribution (Figures 9, 10 and 13) as uniform as possible.

8. Conclusions

The FEM material modeling built on Abaqus/Stardard platform presented here describes Austenite evolution during rolling and decomposition into Multiphase microstructures during cooling. The cooling segment is fully coupled to the Thermo-Mechanics and has been validated at constant (dilatometer) and variable (pilot mill experiments) cooling rates.

The ROT model can simulate cooling rates varying in time and position due to radiation, natural and forced convection. This last is introduced by a sequence of water curtains and nozzles of different geometry, orientation, frontal and backwards boiling water zones defined in an auxiliary file. The strip cooling profile through length, width and thickness can be modified by changing water flow rates, distance between cooling devices, their geometry and their open/close status. Resulting through-length thermal profiles have been validated against an industrial line. Main features of the ROT simulation are:

- The breakdown of constituent phases at different stages of the cooling can be monitored through length, width and thickness, to take early coiling decisions on the achievement of grade and homogeneity of mechanical properties.
- Full coupling of microstructural changes with the Thermo-Mechanics allows quantifying spring back and loss of flatness due to accommodation of residual stresses resulting from differences in shrinkage between neighboring fibers.
- In contrast with the industrial environment, where many variables can change at a time, simulation can analyze the effects of only one or a few parameters at a time and better identify the response in terms of strip quality (mechanical properties and thickness homogeneity, flatness)

9. References

1. Abad R., Fernandez A. I., Lopez B. and Rodriguez-Ibabe J. M., "Interaction between recrystallization and precipitation during multipass rolling in low C Nb-microalloyed steel" ISIJ Int., 41, 2001, p. 1373-1382.
2. Agarwal P. K., Brimacombe J. K., "Mathematical model of heat flow and austenite-pearlite transformation in eutectoid carbon steel rods for wire", Met. Trans. A, ASM & AIME, vol. 12b, pp. 121-33.
3. Anelli E., Application of Mathematical Modelling to Hot Rolling and Controlled Cooling of Wire Rods and Bars, ISIJ Int., vol 32, 1992, N° 3, p. 440-449.
4. Barbero J., Díaz Alvarez J., Diegelmann V., Langellotto L., Bianchi J., Martin D. et al., "Novel Rolling Methods for Advanced High Strength Hot Rolled Steels", Project RFSR-CT-2008-00023, Final Report 2012, to be published by Office for Official Publ. of the E.U. Technical Steel Research Series.
5. Bhattacharya D., "Metallurgical challenges in the development of advanced high strength steels for automotive applications" , Materials Science and Technology Conference, 2010, 3, p. 1804-1817.
6. Bianchi J.H., "Coupling of Microstructural Rate-Effects with the Mechanics of Deformation", Int. Conference COMPLAS'5, D.R.J.Owen, E. Oñate, P Hinton eds., CIMNE eds., Barcelona, 1997, p. 1276-1283.
7. Bianchi J.H., Karjalainen L.P., 'Modelling of dynamic and metadynamic recrystallisation during bar rolling of a medium carbon spring steel', Journal Materials Processing Technologies, 160, 2005, p.267- 277.
8. Bianchi J.H., Vescovo P., "Development and validation of Mechanical Properties Models for Dual Phase Steels". Int. Conf.: New Developments on Metallurgy and Applications of High Strength Steels, Buenos Aires, 2008.
9. Bianchi J. H., Vescovo P., Langellotto L., "Feasibility analysis of local rheological approaches to FEM analysis of Hot Rolling processes (PROMATSIM Phase I),Tenaris Contract PS-0604043540, CSM Report 14418R, 2009.
10. Bianchi J. H., "Rolling: Microstructural Modeling" , Tenaris contract BS-1004160071, CSM Report 15481R, 2011.
11. Cho M., Thomas B.G. Lee P., "Three-Dimensional Numerical Study of Impinging Water Jets in Runout Table Cooling Processes", Met.Mat. Trans. B, 39b, 2008, p 593.
12. Coppola T., Gotti A., Pietrosanti C., Cella A., Mariani F., "Simulazione numerica dei trattamenti termici", XI Convegno Italiano di Meccanica Computazionale, Trento, 1998.
13. Coppola T., Gotti A., "Le interazioni termomeccaniche e metallurgiche nei trattamenti termici degli acciai. Un nuovo modello di calcolo FEM", AIM,Orvieto, 1998.
14. De Moor E., Gibbs P.J. and Speer J. G.,"Strategies for third-generation advanced high-strength steel development", Iron and Steel Technology, 2010, 7 (11), p. 133-144.
15. Di Nunzio P. E., CSM models for grain growth, Internal Communication(2000)
16. Fernandez A. I., Uranga P., Lopez B. andRodriguez-Ibabe J. M., "Static Rrecrystallization behaviour of a wide range of grain sizes in Microalloyed Steels", ISIJ International, Vol. 40, 2000 , 9, p. 893-901.

17. Fernandez A. I., Uranga P., Lopez B. and Rodriguez-Ibabe J. M., “Dynamic recrystallization behaviour covering a wide austenite grain size range in Nb and Nb-Ti microalloyed steels”, Mater. Sci. Eng. A, A361, 2003, p.367-376.
18. Gutierrez I., Parker S., Bianchi J.H., Paul G., Mesplont C., Wojcicki M., et al. “Mechanical Property Models for High Strength Complex Microstructures (MEPMO)”, Report EUR 23181, Off. Official Publ. E.U., Technical Steel Research Series, 2008.
19. Ibrahim M., Shulkosky R., “Simulation and Development of Advanced High Strength Steels on a Hot Strip Mill Using a Microstructure Evolution Model”,HSMM Application for AHSS, 1 , 2007.
20. Jia T., et al. “General method of phase transformation modeling in Advanced High Strength Steels”, ISIJ International, 50 (4), 2010, pp. 583-590.
21. Koistinen D.P., Marburger R.E.: “A general equation prescribing the extent of the austenite-martensite transformation in pure iron-carbon alloys and plain carbon steels”. Acta Metall., 1959, vol. 7, pp. 59-60.
22. Langellotto L., Petrone E., “Finalization of CSM microstructural algorithms implementation” , CSM Report 13464R, Dal-07/94, 2008
23. Langellotto L., Adinolfi S., Illuminati M., Lepore L., “Fabbricazione e Raffreddamento del Lingotto A87 in Acciaio F22+V”, La Metallurgia Italiana, June 2008.
24. Li G.Y, “Development and application of new materials and new technology in heat treatment for auto panels and auto components” Jinshu Rechuli/Heat Treatment of Metals, 2010, 35 (12), p. 1-12
25. Prieto M.M., Ruiz L.S., Menéndez J. A., “Thermal performance of numerical model of hot strip mill runout table”, Ironmaking and Steelmaking”, 2001 Vol. 28 No. 6. p. 475.
26. Roucoules C., Hodgson P., Yue S. and Jonas J.J., 'Softening and microstructural change following the DRX of Austenite', Met. and Mat. Trans. A, 25A, 1994, p. 389-400.
27. Scheil E., “Anlaufzeit der Austenitumwandlung” Arch. Eisenhuttenwes, 1935, vol. 12, pp. 565-567.
28. Sellars C.M., Proc. 7th Int.Symp on Metallurgy and Materials Sci.,N. Hansen et al ed., RISO Nat. Lab., Roskilde, Denmark, 1986,p. 167-187
29. Sellars C.M., “Modelling Microstructural Development During Hot Rolling”, Materials Science and Technology, vol. 6, 1990, p. 1072-1081
30. Sellger R., Hillert M., Bianchi J., Agren J. et al., “Control of phase transformation during processing of partially bainitic multi-component strip steels for controlling the work-hardening characteristics”. Report EUR 20582, Off. Official Publ. E.U., Technical Steel Research Series, 2003.
31. Uranga P., Fernandez A., Lopez B., Rodriguez-Ibabe J.M., Transition between static and metadynamic recrystallization kinetics in coarse Nb microalloyed austenite, Mater. Sci. Eng.. A, 345A , 2003, p.319-327.

10. Acknowledgments

The authors acknowledge financial support from the RFCS Program of the European Union, Contract N° RFSR-CT-2008-00023.